Biomedical Materials & Devices (2023) 1:1009–1021
https://doi.org/10.1007/s44174-023-00069-w

ORIGINAL ARTICLE

Broadening the Utilization of Flexible and Wearable Pressure Sensors for the Monitoring of Health and Physiological Activities

Bijender[1,2] · **Ashok Kumar**[1,2]

Received: 7 February 2023 / Accepted: 3 March 2023 / Published online: 30 March 2023

Abstract

Recently, the high need for artificial intelligence, human motion monitoring, and wearable devices that can be utilized to track human health conditions, particularly for patients experiencing any sickness, has drawn serious interest from researchers. The flexible pressure sensors are a promising possibility for these human–machine interface applications because of their quick reaction, huge sensitivity, and ultra-low detection limit. These flexible sensing devices provide real-time statistics about the conditions of the human body, like blood pressure and heartbeat estimation, to recognize cardiovascular-related diseases. We have developed a versatile and wearable capacitive sensing device by changing the polydimethylsiloxane (PDMS) dielectric layer's structure using a scrubber layer which introduced the porosity in the dielectric layer. The developed sensor showed excellent response under static pressure and dynamic pressure applications. Due to large sensitivity, high working stability, and speedy reaction (120 ms), the versatility of the pressure sensor has been demonstrated in various human motion monitoring applications like wrist bending, palm grip, elbow bending, knee twisting, and vocal-cord vibration detection. In addition, the developed sensor was also used in human–machine interface applications to perceive heartbeat and wrist-pulse motion under typical and after-exercise conditions.

Keywords PDMS · Pressure sensors · Wearable devices · Health monitoring · Human motion monitoring

Introduction

Human blood pressure is an important physiological parameter that must constantly be checked to detect cardiovascular disorders like heart failure and early stroke, which damage vital human organs in the long term [1–3]. A major contributing factor to kidney failure and a leading cause of death worldwide is high blood pressure, often known as hypertension ("the silent killer"). Therefore, it is crucial to monitor blood pressure (BP) in order to pre-diagnose medical conditions and maintain overall good health. In addition to blood pressure, real-time and ongoing physiological signal monitoring is necessary for mobile health, which is growing as a popular technique for effective and convenient medical services [4–6]. In the United States, for instance, about 83% of doctors currently use mobile health approaches to keep an eye on their patients' health [7, 8]. These strategies involve applying various systems to track various physiological signs. Today, flexible and wearable pressure sensors (or flexible electronics) are crucial and can be utilized as human–machine interface devices to monitor human blood pressure and various physiological activities [9]. Therefore, in recent years, there has been an expeditious increase in the demand for flexible electronic technology consisting of electronic skin and wearable devices [10, 11]. Due to their skin-sensing capabilities, electronic skin devices can be used in artificial intelligence, human health, and motion monitoring devices [12–18]. Flexible electronic technology has great potential, by which portable and wearable devices can replace traditional medical diagnostic instruments with convenient features. Conventional healthcare devices include metal-based pressure sensors and rigid semiconductors, which are poorly biocompatible due to their rigidity [19]. The rigid sensors are unsuitable for flexible wearable devices due to their limited sensing range, low sensitivity, and incredibly low flexibility [20]. As a result, flexible wearable and electronic skin devices

✉ Ashok Kumar
ashok553@nplindia.org

[1] CSIR-National Physical Laboratory, Dr. K. S. Krishnan Marg, Delhi 110012, India

[2] Academy of Scientific and Innovative Research (AcSIR), Ghaziabad 201002, India

are predominantly used to upgrade conventional healthcare services for applications, including health monitoring. These healthcare systems gave a new paradigm to the patients to assess or pre-diagnose the illness at any time or place [21]. Flexible and wearable sensing devices play a crucial role in advancing flexible electronic technology due to their distinct advantages, such as low power consumption, high sensitivity, low cost, spectacular working stability, and enormous mechanical flexibility [22–25]. Due to the superior performance of the flexible sensing devices, it fulfills the urgent need in the clinical market for human health/wellness and physiological monitoring devices. Because of their extreme mechanical flexibility, these pressure-sensing devices could be used as wearable devices that can be easily employed in portable medical diagnostic devices for actual tracking of the various human activities personally at home. In addition, Flexible and wearable sensing devices should also be self-powered, self-healing, and able to integrate numerous complicated applications with multiple sensors. But wearable sensing technology still has a long way to go before it can effectively adapt to these applications in terms of quick response [26], high working stability [27], ultra-low detection limit, and strong robustness [28] to adapt practically to these applications. That is why a lot of work is to be done to develop a highly sensitive flexible sensing device that can be applied for the above applications.

In this regard, to date, many researchers have demonstrated a variety of flexible pressure sensors having high sensitivity and high mechanical flexibility based on the piezoresistive [29–34], capacitive [35–42], piezoelectric [43–49], and triboelectric [50–53] transduction mechanisms and they also explored their applications in wearable devices [19, 54–57], electronic skin [5, 27, 58–62], and human physiological monitoring [22, 63–65]. Several review articles on different transduction mechanisms with their fabrication approaches and applications of pressure sensors have been published [12, 20, 66–68]. Out of the existing transduction mechanisms, the sensing devices based on a capacitive transduction mechanism have fast response, low power consumption, ease of processing, high working stability, low hysteresis, and detection limit of ultra-low pressure as compared to sensors based on other mechanisms. Due to these advantages, we have selected capacitive pressure sensors that meet the requirements of monitoring human physiological activities, blood pressure, and heartbeat pulse. In prospect, due to the high flexibility of these sensing devices, respiratory monitoring applications form good contact with the human skin without causing any harm to the human body. So, flexible capacitive pressure sensors are potential candidates compared to other pressure sensors due to their functional advantages and numerous wearable applications.

In capacitive sensors, a dielectric is sandwiched between two parallel conducting plates, and its capacitance is influenced by the thickness of the dielectric layer (d) and the relative area of the electrodes (A). The mathematical representation is given by

$$C = \varepsilon_o A/d$$

where ε_o is the dielectric constant in a vacuum, these sensors' sensitivity is closely correlated with how their capacitance values vary in response to external pressure. As previously stated, the area and thickness of the dielectric layer affect the capacitance value. The sensor's area can be increased, and the value of d can be reduced as much as possible by tweaking the microstructure of the dielectric layer, which will ultimately raise the sensor's sensitivity. In this regard, researchers have done excellent work and improved the sensing device's key parameters by different methods [69–71].

As was already said, a capacitive pressure sensor's performance depends on the features of its elastomeric dielectric layer, which must have high flexibility and elasticity. Due to its great flexibility and elasticity and ability to change its structure to suit the application's needs, polydimethylsiloxane (PDMS) elastomer is a potential candidate for the dielectric layer to develop a capacitive pressure sensor among many other elastomers. PDMS possesses some exciting properties, such as being chemically inert, good thermal stability, high physical toughness, resistance to biodegradation, biocompatibility, and simple fabrication method, and ease of structure modification [72]. These properties make it more suitable for biomedical applications. Over and beyond its benefits, PDMS has a significant drawback in that it cannot produce a tangible link among various metal electrodes. We used an indium-tin-oxide (ITO)-coated polyethylene terephthalate (PET) substrate for electrodes to overcome this drawback. It also has high flexibility and transfers the applied pressure to the PDMS dielectric layer. Changing the PDMS layer's structural layout can significantly enhance a capacitive pressure sensor's performance. We have also developed a capacitive pressure sensor using PDMS as a dielectric layer and ITO-coated PET substrate for flexible electrodes. In the earlier work [39], the PDMS dielectric layer was micro-structurally altered using a scrubber layer to improve its key features.

This paper is an extension of our previous work [39], where the effectiveness of the sensor is increased by increasing the porosity of the PDMS dielectric layer using two layers of a scrubber. First, the sensor was tested under the application of static pressure over a wide pressure range, and simultaneously, the response or recovery characteristics and the device's reliability were investigated. After the device's observed admirable performance, the developed device's applications are extended into human health monitoring like wrist-pulse, heartbeat, and blood pressure measurement at normal and after-exercise conditions. The sensor

also monitored human physiological activities like palm grip, vocal-cord vibration, vocal motion during swallowing, wrist, elbow, and knee bending. Due to magnificent sensitivity and application in human state motion recognition, the developed sensing device shows its potential for E-skin and robotic applications.

Experimental Section

Fabrication of the Pressure Sensor

The sensor was fabricated the same way we had done in the earlier reported work [39]. However, there was a slight change in the fabrication process to increase the porosity of the dielectric layer. In this work, two layers of scrubber (thick layer) were taken instead of a single layer to create more porosity, and further, it was used in the formation of a dielectric layer. The thick layer of the scrubber was coated with a 10:1 mixture of PDMS and its curing agent, which was then solidified by annealing it at 100 °C for 2 h. After the curing procedure, the PDMS-Scrubber layer was removed from the petri dish and used as a dielectric layer (thickness—2.6 mm and dimension—18 mm × 18 mm) by sandwiching it between the flexible electrodes to develop the pressure sensor. The preceding reported work gave the schematic representation of the sensor's fabrication process.

Characterization of Dielectric Layer and Measurements

A scanning electron microscope (Zeiss EVO 18) at 15 kV and a digital microscope (Celestron microscope) were used to study the surface morphology of the prepared dielectric layer. The microscopic and optical images of the PDMS-Scrubber layer taken by the above microscopes confirmed the presence of the large pores in the form of voids.

The static pressure measurement, response, recovery time characteristics, working stability, and the prepared device's applications were performed at atmospheric conditions with an impedance analyzer (HIOKI 3532-50 LCR Hi-tester). The value of the applied pressure depended only on the mass of the dead weights because the effective area of the device was fixed. In order to maintain the device's effective area during the static pressure measurement, a glass plate of optimized dimension 12 mm × 12 mm was used, and the external pressure was applied by placing the self-made dead weights on the glass slide. The dead weights are traceable to mass standards and area from dimension metrology. The variation in the capacitance values was observed under the exterior pressure ranging from 10 Pa to 54 kPa at a frequency of 1 MHz. Similarly, for actual tracking of human health and physiological actions, the sensor responds in terms of change in the capacitance values during the motion of human body parts at different angles.

Results and Discussion

Characterization and Performance of the Sensor

As said earlier, the preparation method of the sensor was the same as reported in the preceding work, with a slight difference in that there was a two-layer scrubber incorporated in the PDMS layer to enhance the porosity [39]. The prepared micro-structured dielectric layer dimension was 2.6 mm thick and 18 mm × 18 mm. Figure 1 shows the scanning electron microscopic and optical images of the prepared dielectric layer, taken by SEM and digital microscope. The side-view SEM images of the PDMS-Scrubber layer (porous PDMS layer) clearly show the presence of large pores, as shown in Fig. 1a and b. Figure 1c and d represents the top and side-view optical images of the developed layer, and they also show the presence of the pores in terms of voids and bubbles.

The prepared sensor was tested under static pressure conditions, similar to our previous work [39]. The experimental setup and the conditions were the same as the earlier reported work. A schematic diagram of the experimental setup is given in Fig. 2a. But in this work, the sensor showed a more significant change in the capacitance values due to increased porosity in the elastomeric layer when the external pressure was applied. The fabricated device offers a relative change of 0.1% and 55% in capacitance values for 10 Pa and 54 kPa pressure, respectively (as represented in Fig. 2). In contrast, the preceding sensor showed only 0.03% and 23.76% for 10 Pa and 54 kPa pressure. The sensor exhibited approximately a linear behavior with the external pressure over a wide range (from 10 Pa to 54 kPa), as given in Fig. 3a.

There was an increment in the sensor's sensitivity over the entire pressure domain compared to the earlier developed sensor. The prepared device showed the sensitivity (%) of 0.017 Pa^{-1} and 0.021 Pa^{-1} for the pressure range of 10 Pa to 50 Pa and 100 Pa to 500 Pa (as illustrated in Fig. 3b and c), which is approximately four times more in comparison with preceding sensor. The sensor also showed better sensitivity in the pressure domain of 5 kPa to 30 kPa, which was 7.94×10^{-4} kPa^{-1}, as represented in Fig. 3d.

After getting good results for the static pressure measurement, the sensor's working stability was tested under pressure for a long time with the help of dead weights to check its performance for long time. The sensor showed a negligible change in capacitance values for nearly an hour at various pressure values of 100 Pa, 500 Pa, 5 kPa, and 30 kPa, which confirmed the high operational stability of the device, and the sensor can work for a long time without loss

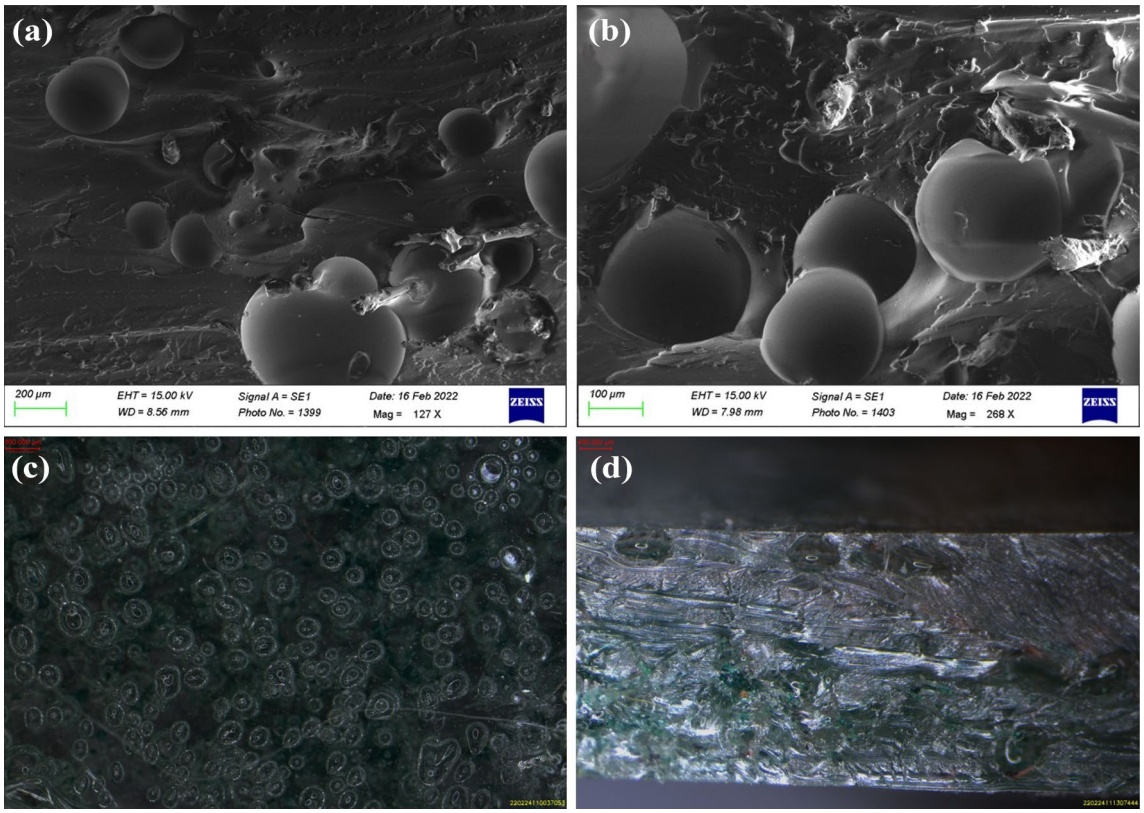

Fig. 1 **a** and **b** SEM images of the fabricated micro-structured dielectric layer (PDMS-Scrubber) from the side-view indicate the porosity in terms of many pores inside it. **c** and **d** An optical microscopic image of the porous PDMS layer also confirmed the residence of the pores in terms of voids and air bubbles

in the output signal (as represented in Fig. 4a). Besides this, the time consumption by the sensor during the response and recovery process was also calculated by loading or unloading the weights on the sensor, as illustrated in Fig. 4b. It was found that the sensor responded very quickly with a response time of 120 ms and also recovered speedily with a time of 120 ms when the weight was lifted off, within the limitation of the time used for mechanical loading and unloading of the sensor by using dead weights.

The fabricated sensing device responded very well under the static pressure applied from 10 Pa to 54 kPa and showed high sensitivity, quick response, and high working stability. A comparative study between the key parameters of the developed sensor with our previous sensor and other existing PDMS-based sensor is given in Table 1.

To check the suitability of the developed device for blood pressure monitoring applications, first, its performance should be checked under the influence of the pressure in terms of mmHg, whether its response or not in the range of human blood pressure. In this regard, the response of the sensor was recorded under the external pressure, which was in terms of mmHg rather than in Pa. The range of the external pressure was chosen in such a way that it can include the complete blood pressure (BP) range (i.e., low, standard, and high BP) of humans. The pressure was applied from 50 to 240 mmHg in the forward and reverse directions with the help of non-invasive blood pressure (NIBP) analyzer. Again, the sensor shows an outstanding response to applying pressure in forward and reverse trends as it had done in static pressure measurement. There was approx. 20% and 53% relative difference in the capacitance for 50 mmHg and 240 mmHg pressure values, respectively. The sensor showed almost a linear behavior with the applied pressure in the forward and reversed direction. It was found that the response curves completely overlap each other, proving the sensor's reliability. The sensitivity in terms of mmHg of the sensor was obtained by the slope of the graph between the changes in capacitance values ($\Delta C/C_0$) and the varying external pressure from 50 to 240 mmHg that was of 0.16 $mmHg^{-1}$, as shown in Fig. 5c.

Applications

According to the explanation in section "Characterization and Performance of the Sensor" above, the developed sensing device exhibits outstanding sensitivity, rapid

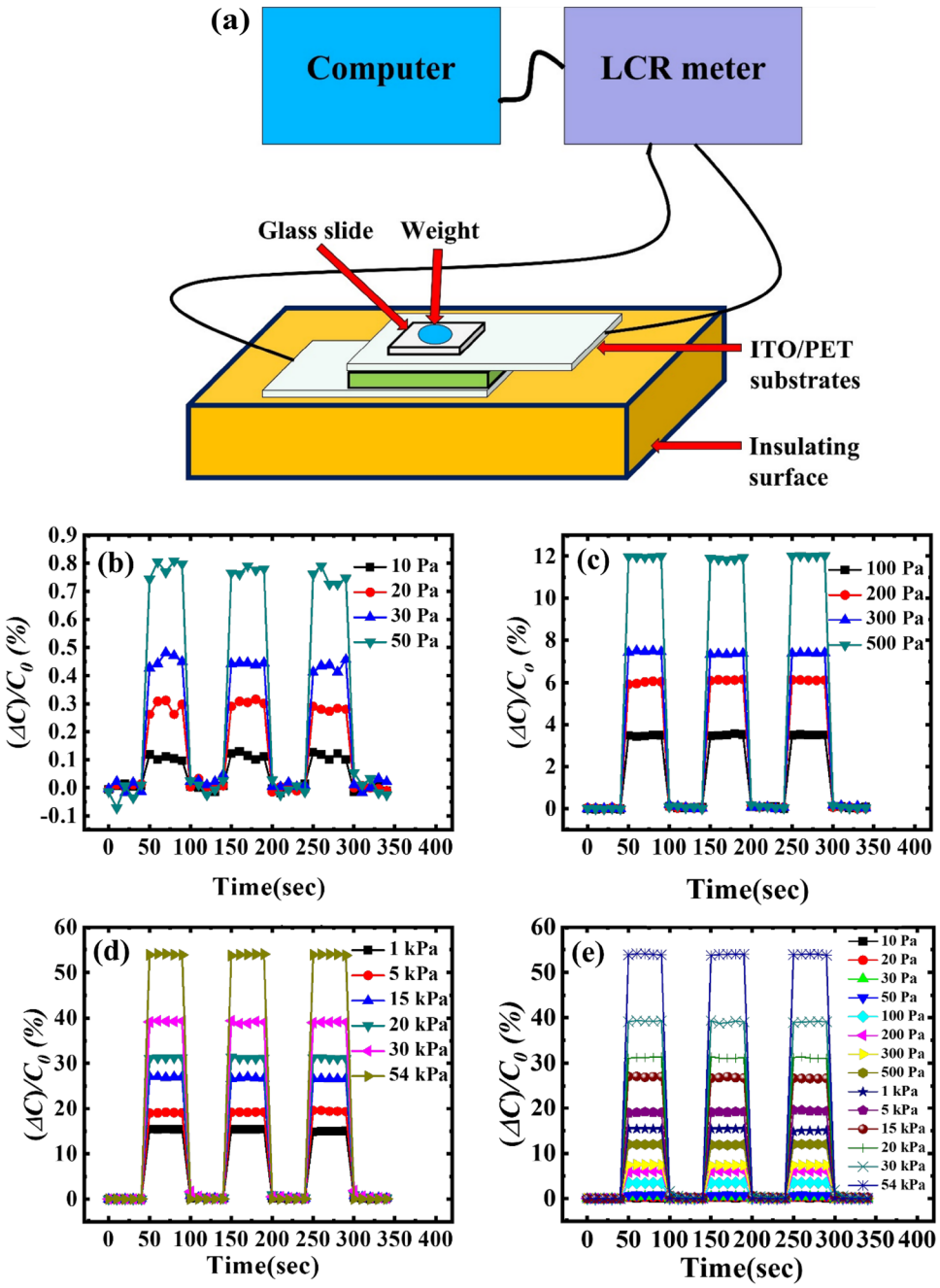

Fig. 2 The output response of the fabricated sensor in respect of capacitance values($\Delta C/C_0$) with the schematic diagram of the measurement setup **a** under the application of static pressure ranges from **b** 10–50 Pa. **c** 100–500 Pa. **d** 1–54 kPa and **e** 10 Pa to 54 kPa

response to applying pressure, and good functioning stability. When the sensor was tested for static pressure in the 50 to 240 mmHg range of human blood pressure, it responded immensely to the applied pressure. Due to its exceptional performance, the sensing device was examined for its numerous applications in monitoring human health and physiological activities, which will be discussed in this section. All the experiments for tracking physiological activity and health were conducted on the author's body. By acknowledging this, the author agrees that all the experiments were performed on his body and that no other person was harmed during these demonstrations.

First, under regular and post-exercise situations, wearable real-time wrist-pulse and heartbeat monitoring was demonstrated. The sensor's capacitance variations owing to undesired signals or noise were measured before monitoring wrist pulse and heartbeat accurately by fastening the sensor to a person's palm. The sensor showed an approximate 1.5% relative change in capacitance value as noise or undesired signal, as shown in Fig. 6e. The developed sensor

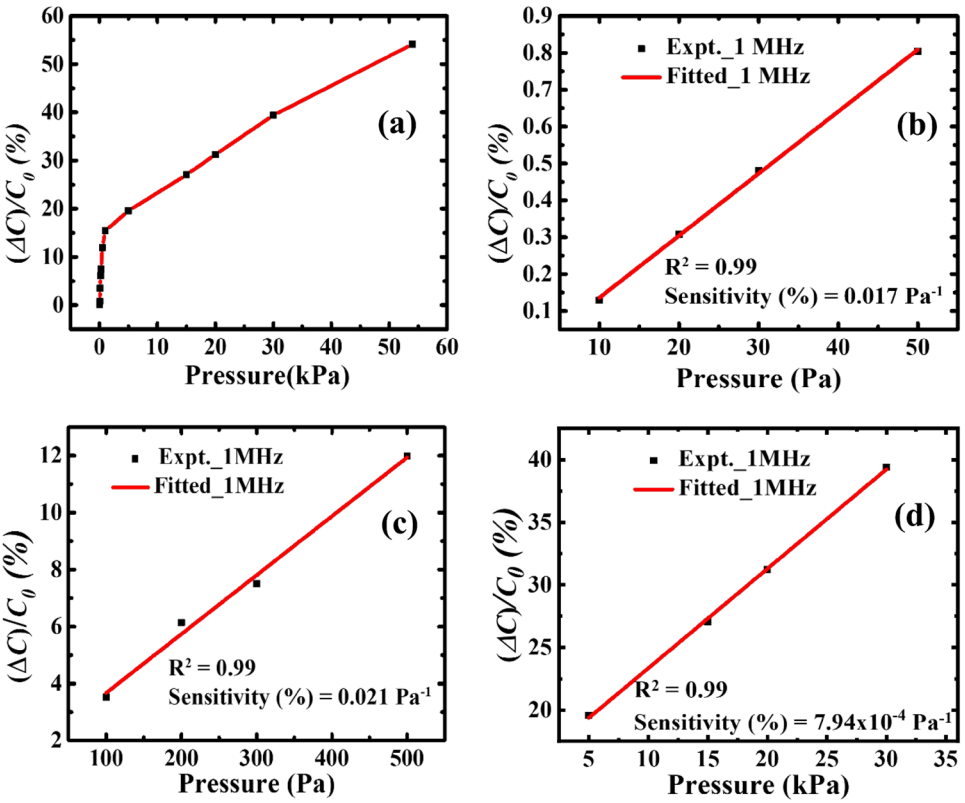

Fig. 3 The capacitive sensing characteristics of the developed sensor for the external static pressure region of **a** 10 Pa to 54 kPa. **b** 10–50 Pa. **c** 100–500 Pa and **d** 5–30 kPa

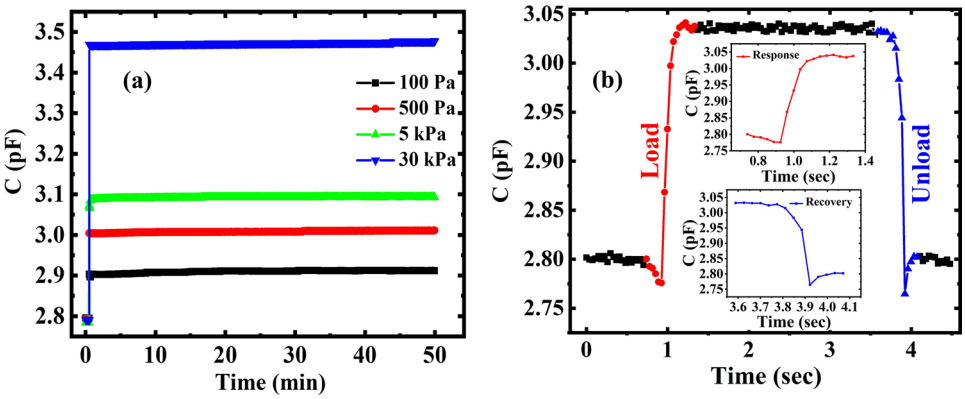

Fig. 4 **a** The sensor's operating stability test under the external pressure of 100 Pa, 500 Pa, 5 kPa, and 30 kPa. **b** The capacitance response or recovery curve for the developed sensing device during loading or unloading of pressure

Table 1 A comparison between the key parameters of capacitive pressure sensors with developed sensor (bold letters)

Mechanism	Material/structure	Sensitivity (Pressure range)	Lowest detection	Response/recovery time	References
Capacitive	PDMS/Wrinkled microstructure	0.0012 kPa^{-1} (< 1 kPa) 4.2×10^{-6} kPa^{-1} (> 8 kPa)	–	578/782 ms	[73]
Capacitive	Microporous PDMS	0.28 kPa^{-1}	38.8 Pa	340 ms	[74]
Capacitive	Bubble trapped PDMS	5.5×10^{-3} kPa^{-1}	–	~350/385 ms	[75]
Capacitive	PDMS/microstructure	0.1 kPa^{-1} (< 12 kPa)	–	190/- ms	[76]
Capacitive	PDMS/microstructure	0.0046 Pa^{-1} (< 0.05 kPa) 0.0051 Pa^{-1} (< 0.5 kPa)	~5 Pa	–	[39]
Capacitive	**PDMS/microstructure**	**0.017 Pa^{-1} (< 0.05 kPa)** **0.021 Pa^{-1} (< 0.5 kPa)**	**10 Pa**	**120/120 ms**	**This work**

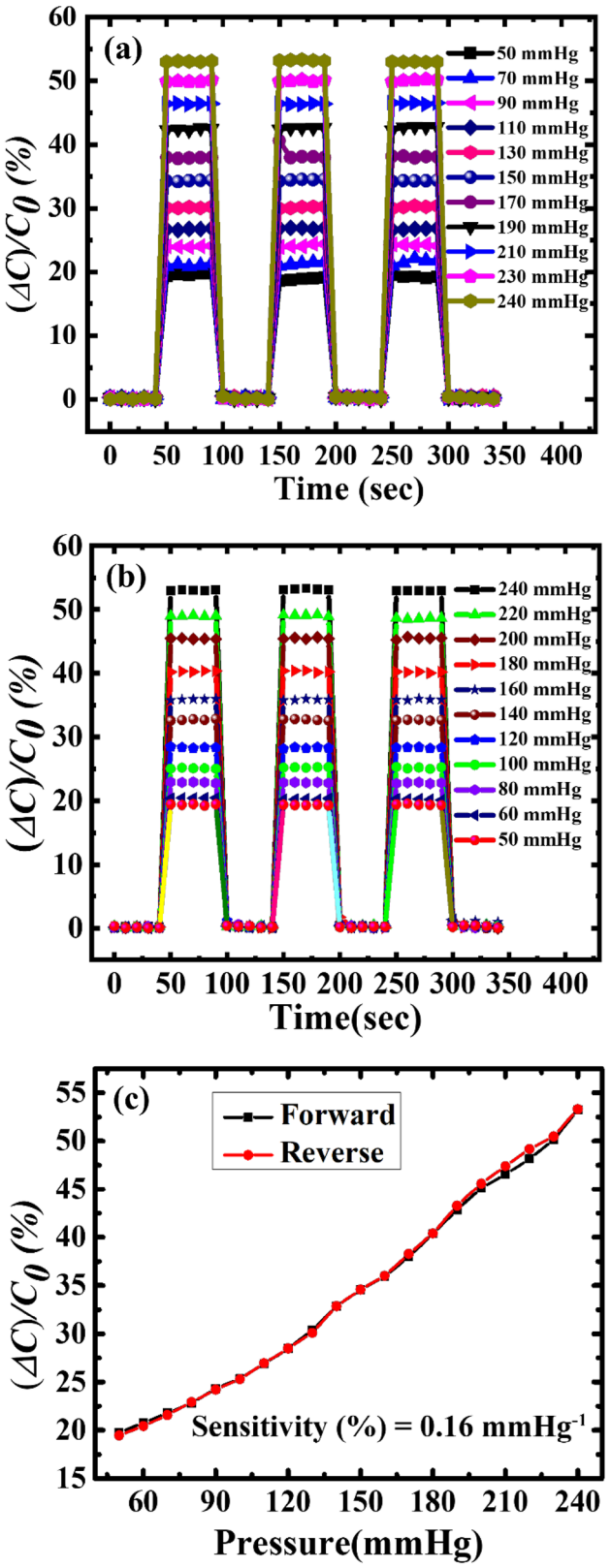

Fig. 5 **a** and **b** The capacitance response curve of the sensor at numerous external pressure values ranging from 50 to 240 mmHg in forward and reverse directions using the NIBP simulator. **c** The pressure response curve of the sensor with porous PDMS layer in both directions of external pressure varies from 50 to 240 mmHg

was attached to a person's wrist for wrist-pulse monitoring (see inset of Fig. 6), and the output signal was measured in the form of capacitance values using an impedance analyzer. The sensor manifested a relative change of approx. 9% in the capacitance value at standard conditions, with a relative change of approx. 20% after exercise, as given in Fig. 6a and b. As we know, after exercise, the flow of blood increases in the human body, which exerts more pressure on the wall of arteries/veins, and our advanced sensor tracked that exerted pressure very well. Figure 6b demonstrates that the sensor exhibits a 20% relative change after exercise and that the variation in capacitance value reduced as the person relaxed. The difference in capacitance value returns to around 9% when the human is completely relaxed, and the same as for the normal condition. Similar to this, the heartbeat was also tracked by placing the sensor on a human's chest (inset of Fig. 6), and a relative change of around 10% was seen when the subject was at ease or in a normal state (as shown in Fig. 6c). After exercise, the capacitance value changed relatively by around 23%, which is more than twice as much as under normal circumstances. So, in both cases, the designed device immediately detects changes in blood flow and heartbeat (regular and after exercise).

On behalf of these good results from the wrist-pulse and heartbeat monitoring, the fabricated sensor proved its capability for some more advanced applications. So, the developed sensing device was tested for human blood pressure monitoring under relaxed and after-exercise conditions. Because blood pressure monitoring for humans is vital, especially for patients suffering from cardiovascular and kidney diseases. For blood pressure monitoring, the sensor was attached to the elbow of the human, and a cuff was wrapped over the hand above the sensor, which was connected to the OMRON blood pressure machine (as shown in Fig. 7a). The OMRON machine applied the pressure in the cuff until blood flow was nearly blocked in the human arteries/veins and then decreased the pressure slowly until fully vented. The fabricated sensor senses the blood flow in the human artery/vein during the process, and the sensor output is measured as a capacitance value from the impedance analyzer. As we can see in Fig. 7b and c, when the OMRON started to apply the pressure, the capacitance value of the sensor increased because the pressure near the cuff was more due to the cuff's inflation, and the sensor got maximum capacitance value when full pressure was applied in the cuff. After that, the capacitance value decreased with the pressure decrease in the cuff. Along with this envelope, there were fluctuations due to blood flow concerning systolic and diastolic pressure. The fluctuations concerning systolic and diastolic were more for exercise conditions (153–85) than for the relaxed state (118–78). This happened because of the high blood flow speed after exercise and due to which more fluctuations were obtained in the envelope, as represented

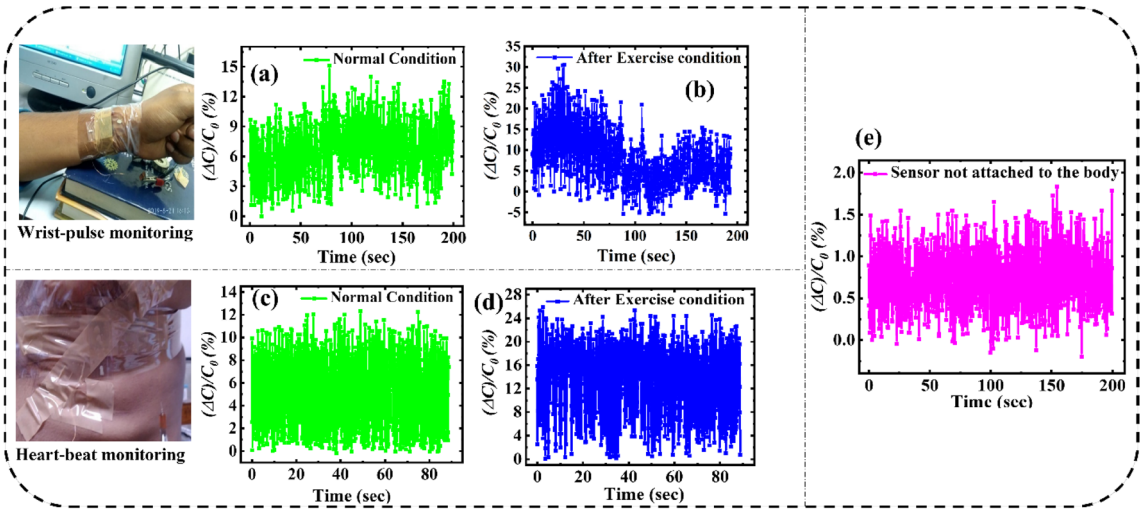

Fig. 6 **a** and **b** Wrist-pulse monitoring using the sensor at normal and after-exercise conditions. **c** and **d** The device is mounted on the chest for heartbeat monitoring in relaxed and after-exercise conditions. **e** The capacitance response of the sensor when the sensor was attached to the palm of the human body

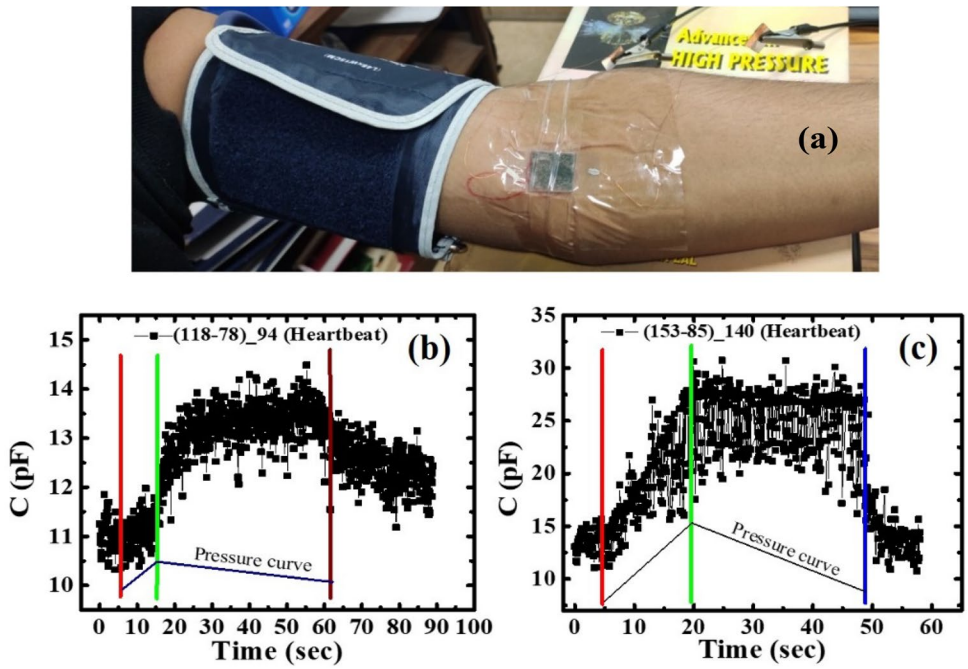

Fig. 7 Real-time response of the developed sensing device for human blood pressure monitoring at **b** relaxed or normal, **c** after exercise. (**a** Image of the sensor placed on the elbow)

in Fig. 7b and c. The fabricated device detects the complete envelope used for systolic and diastolic blood pressure calculation in normal and exercise conditions.

To demonstrate the feasibility of the developed device in the portable and wearable electronic sensor, a sequence of demonstrations is done to detect the various human joint-motion activities like palm grip, wrist bending, elbow bending, knee bending, and vocal-cord motion or vibration, as given in Fig. 8a–e. First, the designed sensor was placed on the human's wrist to detect the gripping and open activity of the palm (Fig. 8a), which could be helpful for physical training. As shown in Fig. 8b, the sensing performance of the sensor is recorded for the bending motion of the wrist at different angles on the upper side by attaching the device to the wrist joint of the human body. The sensor gives different capacitance values for the different angles. The capacitance value increases with increasing angle as pressure increases with the wrist bending on the upper side.

Further, the bending motion of the elbow is also tracked by placing the sensor on the elbow joint, and the elbow is

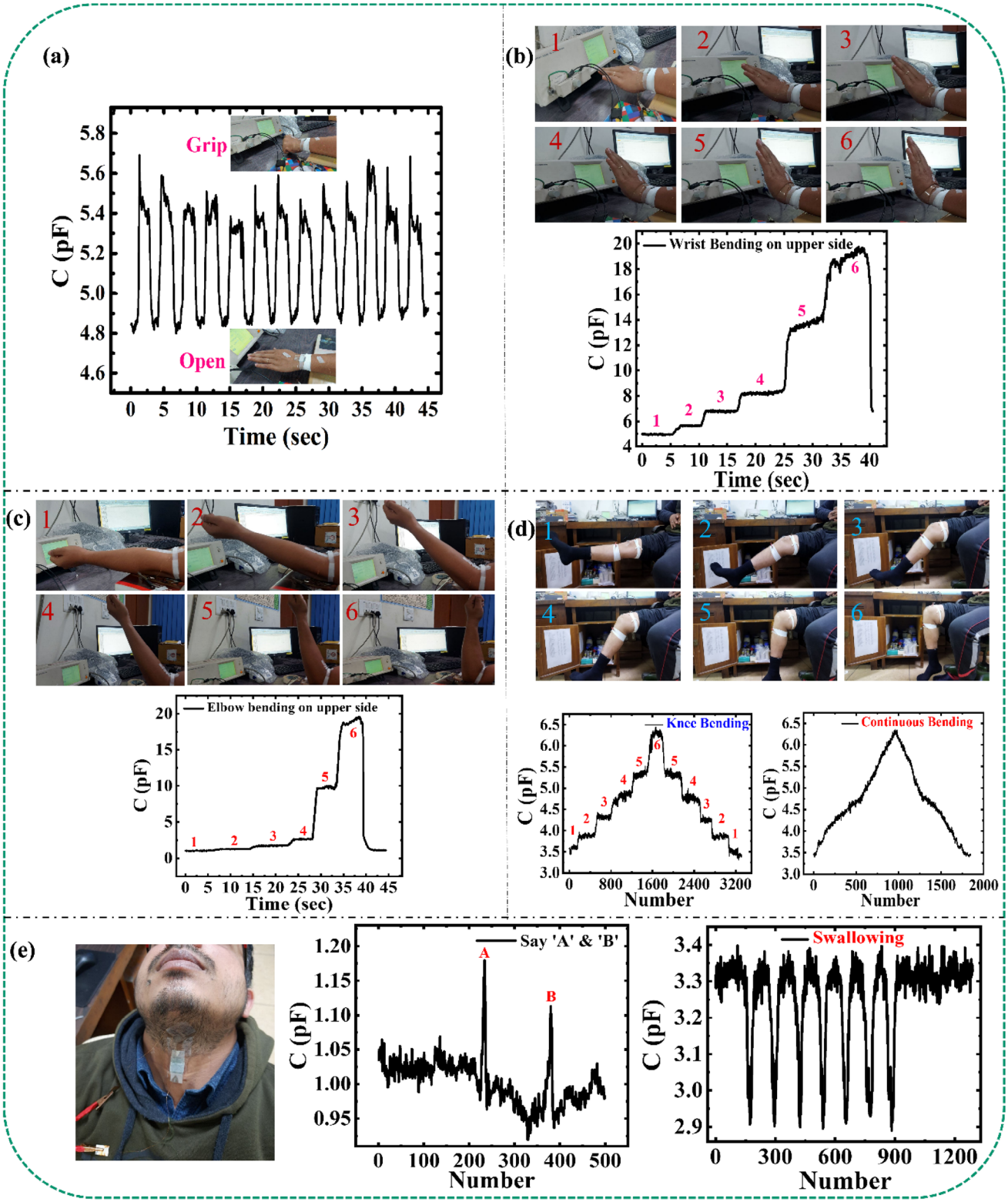

Fig. 8 The developed porous sensing device demonstrated various potential human state motion recognition applications. **a** The sensing performance of the sensor during the gripping and open activity of the human palm. **b–d** The device's real-time response to detect the wrist, elbow, and knee bending at five different angles (inset: photograph of the sensor attached to the wrist, elbow, and knee joint of the human body). **e** The device was mounted on the vocal cord to detect voice signals while pronouncing 'A' and 'B' and the motion of the throat during swallow activity

bent at five different angles up to a maximum of 90°, as given in Fig. 8c. Similarly, the device shows five different capacitance values for the five different bending angles of the elbow. At small angles, the human body exerts little pressure (due to strain in muscles) on the sensor, so there was a minor change in capacitance value. But, at approx. 60° and 90° angles, the human body exerted more pressure (at these angles, the sensor was sandwiched between the lower and upper arm), and due to that, there was a rapid increase in the capacitance response of the device. Therefore, it has been said that the PDMS-scrubber sensor can be used to distinguish between different orientations of wrist and elbow movements.

Figure 8d presents the response of the capacitance signal of the sensor for the bending motion of the human knee at five different angles in both directions: (1) from 0 to 90° angle and (2) from 90 to 0° angle. The sensor is attached to the knee joint to track its motion, giving different capacitance values for different angles, with a maximum value at an angle of 90°. At an angle of 90°, the maximum strain was applied to the sensor due to the complete bending of the knee, and the sensor was in a bent shape, which resulted in a sharp increase in the capacitance value. The continuous bending of the knee in forward and reverse directions was also tracked, as shown in Fig. 8d. Thus, the sensor could monitor knee injuries or movement during running.

Furthermore, the porous sensor was attached to the vocal cord/throat to record the voice signal during the pronunciation of the alphabet and swallow activity, as illustrated in Fig. 8e. Clear spikes were presented in the sensor's capacitance response while pronouncing the alphabets 'A' and 'B.' During swallowing, the sensor's capacitance was decreased from 3.3 to 2.9 pF. This happens because while swallowing, the throat goes inside for some instant, and at that time, the sensor has relaxed from the attachment to the throat, which increases the thickness of the dielectric layer (d) because it was little pressed during attachment by adhesive tape on it. Due to an increase in the d value, the capacitance of the sensor was decreased during the activity. Thus, all these demonstrations highlighted that the PDMS-Scrubber sensor has great potential for usage in various human health and motion detection applications. These promising applications of the developed device make it suitable for human–machine interface, electronic skin, and robotic skin applications.

Conclusion

In conclusion, we have developed a capacitive pressure sensor using PDMS as a dielectric layer. The porosity was introduced at a large scale in the PDMS layer using scrubber layers to boost the sensor's performance. Cross-sectional SEM and optical microscopic images confirmed the existence of pores in the elastomeric layer. The porous sensor showed remarkable sensitivity of 0.017 Pa^{-1} in a pressure range of 10 Pa to 50 Pa and 0.021 Pa^{-1} in 100 Pa to 500 Pa. The sensor illustrates great potential for low-pressure detection, high operational stability, linear response over a wide operating pressure range, and a reasonable response time of 120 ms. The pressure sensor results in static pressure measurement suggest possible uses as a wearable pressure-sensing device for various applications, including wrist-pulse, heartbeat, and blood pressure measurements. The sensing device also detected human body motions like palm gripping, wrist bending, elbow bending, knee bending, and vocal-cord vibrations. Hence, due to the simple fabrication method and great sensing performance in static and dynamic pressure measurement, the developed sensor proved the potential for human health monitoring, detection of human motions, electronic skin, and robotic skin applications.

Acknowledgements The authors thank the Director, CSIR-NPL and Head, Physico-Mechanical Metrology division, CSIR-NPL, for their support and constant encouragement. Mr. Bijender would like to acknowledge AcSIR and CSIR-NPL for allowing me to pursue Ph.D. and CSIR, India. The authors also thank Mr. Shubham Kumar for his help and support.

Data Availability The data that supports the findings of this study are available from the corresponding author on request.

Declarations

Competing Interests The authors declare that they have no known competing financial interests or personal relationships that could have appeared to influence the work reported in this paper.

References

1. W.B. Kannel, Blood pressure as a cardiovascular risk factor: prevention and treatment. JAMA **275**, 1571–1576 (1996). https://doi.org/10.1001/JAMA.1996.03530440051036
2. S. MacMahon, R. Peto, R. Collins, J. Godwin, S. MacMahon, J. Cutler, P. Sorlie, R. Abbott, R. Collins, J. Neaton, R. Abbott, A. Dyer, J. Stamler, Blood pressure, stroke, and coronary heart disease: part 1, prolonged differences in blood pressure: prospective observational studies corrected for the regression dilution bias. Lancet **335**, 765–774 (1990). https://doi.org/10.1016/0140-6736(90)90878-9
3. N. Luo, W. Dai, C. Li, Z. Zhou, L. Lu, C.C.Y. Poon, S.C. Chen, Y. Zhang, N. Zhao, Flexible piezoresistive sensor patch enabling ultralow power cuffless blood pressure measurement. Adv. Funct. Mater. **26**, 1178–1187 (2016). https://doi.org/10.1002/ADFM.201504560
4. Y. Chu, J. Zhong, H. Liu, Y. Ma, N. Liu, Y. Song, J. Liang, Z. Shao, Y. Sun, Y. Dong, X. Wang, L. Lin, Y. Chu, H. Liu, J. Liang, X. Wang, L. Lin, J. Zhong, Y. Ma, N. Liu, Y. Song, Z. Shao, L. Lin Berkeley Sensor, A. Center, Y. Sun, Y. Dong, Human pulse diagnosis for medical assessments using a wearable piezoelectret sensing system. Adv. Funct. Mater. **28**, 1803413 (2018). https://doi.org/10.1002/ADFM.201803413

5. Y. Liu, M. Pharr, G.A. Salvatore, Lab-on-skin: a review of flexible and stretchable electronics for wearable health monitoring. ACS Nano **11**, 9614–9635 (2017). https://doi.org/10.1021/ACSNANO.7B04898/ASSET/IMAGES/LARGE/NN-2017-04898T_0009.JPEG
6. C. Free, G. Phillips, L. Galli, L. Watson, L. Felix, P. Edwards, V. Patel, A. Haines, The effectiveness of mobile-health technology-based health behaviour change or disease management interventions for health care consumers: a systematic review. PLoS Med **10**, e1001362 (2013). https://doi.org/10.1371/JOURNAL.PMED.1001362
7. H. Ouyang, J. Tian, G. Sun, Y. Zou, Z. Liu, H. Li, L. Zhao, B. Shi, Y. Fan, Y. Fan, Z.L. Wang, Z. Li, Self-powered pulse sensor for antidiastole of cardiovascular disease. Adv. Mater. **29**, 1703456 (2017). https://doi.org/10.1002/ADMA.201703456
8. H. Ota, M. Chao, Y. Gao, E. Wu, L.C. Tai, K. Chen, Y. Matsuoka, K. Iwai, H.M. Fahad, W. Gao, H.Y.Y. Nyein, L. Lin, A. Javey, 3D printed "earable" smart devices for real-time detection of core body temperature. ACS Sens. **2**, 990–997 (2017). https://doi.org/10.1021/ACSSENSORS.7B00247/ASSET/IMAGES/LARGE/SE-2017-00247T_0005.JPEG
9. S. Kumar, S. Yadav, A. Kumar, Oscillometric waveform evaluation for blood pressure devices. Biomedical Engineering Advances **4**, 100046 (2022). https://doi.org/10.1016/J.BEA.2022.100046
10. C. Wang, C. Wang, Z. Huang, S. Xu, Materials and structures toward soft electronics. Adv. Mater. **30**, 1801368 (2018). https://doi.org/10.1002/ADMA.201801368
11. A. Nathan, A. Ahnood, M.T. Cole, S. Lee, Y. Suzuki, P. Hiralal, F. Bonaccorso, T. Hasan, L. Garcia-Gancedo, A. Dyadyusha, S. Haque, P. Andrew, S. Hofmann, J. Moultrie, D. Chu, A.J. Flewitt, A.C. Ferrari, M.J. Kelly, J. Robertson, G.A.J. Amaratunga, W.I. Milne, Flexible electronics: the next ubiquitous platform. Proc. IEEE **100**, 1486–1517 (2012). https://doi.org/10.1109/JPROC.2012.2190168
12. W. Chen, X. Yan, Progress in achieving high-performance piezoresistive and capacitive flexible pressure sensors: a review. J. Mater. Sci. Technol. **43**, 175–188 (2020). https://doi.org/10.1016/J.JMST.2019.11.010
13. X. Wang, L. Dong, H. Zhang, R. Yu, C. Pan, Z.X. Lin Wang Wang, L. Dong, H. Zhang, C.F. Pan, Z.L. Wang, R. Yu, Recent progress in electronic skin. Adv. Sci. **2**, 1500169 (2015). https://doi.org/10.1002/ADVS.201500169
14. C. Wang, K. Xia, H. Wang, X. Liang, Z. Yin, Y. Zhang, Advanced carbon for flexible and wearable electronics. Adv. Mater. **31**, 1801072 (2019). https://doi.org/10.1002/ADMA.201801072
15. Z. Lou, L. Wang, G. Shen, Recent advances in smart wearable sensing systems. Adv. Mater. Technol. **3**, 1800444 (2018). https://doi.org/10.1002/ADMT.201800444
16. B.S. Sreeja, R. Sankararajan, Bio-compatible piezoelectric material based wearable pressure sensor for smart textiles. Smart Mater. Struct. (2022). https://doi.org/10.1088/1361-665X/AC9FFA
17. Q. Zhang, W. Jia, C. Ji, Z. Pei, Z. Jing, Y. Cheng, W. Zhang, K. Zhuo, J. Ji, Z. Yuan, S. Sang, Flexible wide-range capacitive pressure sensor using micropore PE tape as template. Smart Mater. Struct. **28**, 115040 (2019). https://doi.org/10.1088/1361-665X/AB4AC6
18. R. Zheng, Y. Wang, Z. Zhang, Y. Zhang, J. Liu, High sensitivity and broad detection range flexible capacitive pressure sensor based on rGO cotton fiber for human motion detection. Smart Mater. Struct. **31**, 025019 (2021). https://doi.org/10.1088/1361-665X/AC3C07
19. X. Wang, Z. Liu, T. Zhang, Flexible sensing electronics for wearable/attachable health monitoring. Small **13**, 1602790 (2017). https://doi.org/10.1002/SMLL.201602790
20. X. Wang, J. Yu, Y. Cui, W. Li, Research progress of flexible wearable pressure sensors. Sens. Actuators A **330**, 112838 (2021). https://doi.org/10.1016/J.SNA.2021.112838
21. G. Schwartz, B.C.K. Tee, J. Mei, A.L. Appleton, D.H. Kim, H. Wang, Z. Bao, Flexible polymer transistors with high pressure sensitivity for application in electronic skin and health monitoring. Nat. Commun. **4**, 1859 (2013). https://doi.org/10.1038/ncomms2832
22. B. Wang, C. Liu, Y. Xiao, J. Zhong, W. Li, Y. Cheng, B. Hu, L. Huang, J. Zhou, Ultrasensitive cellular fluorocarbon piezoelectret pressure sensor for self-powered human physiological monitoring. Nano Energy **32**, 42–49 (2017). https://doi.org/10.1016/J.NANOEN.2016.12.025
23. T. Someya, T. Sekitani, S. Iba, Y. Kato, H. Kawaguchi, T. Sakurai, A large-area, flexible pressure sensor matrix with organic field-effect transistors for artificial skin applications. Proc. Natl. Acad. Sci. USA **101**, 9966–9970 (2004). https://doi.org/10.1073/PNAS.0401918101
24. C. Wang, D. Hwang, Z. Yu, K. Takei, J. Park, T. Chen, B. Ma, A. Javey, User-interactive electronic skin for instantaneous pressure visualization. Nat. Mater. **12**, 899–904 (2013). https://doi.org/10.1038/nmat3711
25. Y. Zang, F. Zhang, D. Huang, X. Gao, C.A. Di, D. Zhu, Flexible suspended gate organic thin-film transistors for ultra-sensitive pressure detection. Nat. Commun. **6**, 6269 (2015). https://doi.org/10.1038/ncomms7269
26. D. Jiang, Y. Wang, B. Li, C. Sun, Z. Wu, H. Yan, L. Xing, S. Qi, Y. Li, H. Liu, W. Xie, X. Wang, T. Ding, Z. Guo, Flexible sandwich structural strain sensor based on silver nanowires decorated with self-healing substrate. Macromol. Mater. Eng. **304**, 1900074 (2019). https://doi.org/10.1002/MAME.201900074
27. X. Tang, C. Wu, L. Gan, T. Zhang, T. Zhou, J. Huang, H. Wang, C. Xie, D. Zeng, Multilevel microstructured flexible pressure sensors with ultrahigh sensitivity and ultrawide pressure range for versatile electronic skins. Small **15**, 1804559 (2019). https://doi.org/10.1002/SMLL.201804559
28. J. Wang, J. Jiu, M. Nogi, T. Sugahara, S. Nagao, H. Koga, P. He, K. Suganuma, A highly sensitive and flexible pressure sensor with electrodes and elastomeric interlayer containing silver nanowires. Nanoscale **7**, 2926–2932 (2015). https://doi.org/10.1039/C4NR06494A
29. A.T. Sepúlveda, R. Guzman de Villoria, J.C. Viana, A.J. Pontes, B.L. Wardle, L.A. Rocha, Full elastic constitutive relation of non-isotropic aligned-CNT/PDMS flexible nanocomposites. Nanoscale **5**, 4847 (2013). https://doi.org/10.1039/c3nr00753g
30. D.J. Lipomi, M. Vosgueritchian, B.C.K. Tee, S.L. Hellstrom, J.A. Lee, C.H. Fox, Z. Bao, Skin-like pressure and strain sensors based on transparent elastic films of carbon nanotubes. Nat Nanotechnol. **6**, 788–792 (2011). https://doi.org/10.1038/nnano.2011.184
31. J. Bae, Y. Hwang, S. Park, J.-H. Ha, H. Kim, A. Jang, J. An, C.-S. Lee, S.-H. Park, Study on the sensing signal profiles for determination of process window of flexible sensors based on surface treated PDMS/CNT composite patches. Polymers (Basel) **10**, 951 (2018). https://doi.org/10.3390/polym10090951
32. C. Pang, G.Y. Lee, K.T. Il, S.M. Kim, H.N. Kim, S.H. Ahn, K.Y. Suh, A flexible and highly sensitive strain-gauge sensor using reversible interlocking of nanofibres. Nat. Mater. **11**, 795–801 (2012). https://doi.org/10.1038/nmat3380
33. D. Wei, X. Song, T. Sun, J. Yang, L. Yu, D. Wei, L. Fang, B. Lu, C. Du, Direct growth of graphene films on 3D grating structural quartz substrates for high-performance pressure-sensitive sensors. ACS Appl. Mater. Interfaces **8**, 16869–16875 (2016). https://doi.org/10.1021/acsami.6b04526
34. C.L. Choong, M.B. Shim, B.S. Lee, S. Jeon, D.S. Ko, T.H. Kang, J. Bae, S.H. Lee, K.E. Byun, J. Im, Y.J. Jeong, C.E. Park, J.J. Park, U.I. Chung, Highly stretchable resistive pressure

sensors using a conductive elastomeric composite on a micro-pyramid array. Adv. Mater. **26**, 3451–3458 (2014). https://doi.org/10.1002/ADMA.201305182
35. C. Metzger, E. Fleisch, J. Meyer, M. Dansachmüller, I. Graz, M. Kaltenbrunner, C. Keplinger, R. Schwödiauer, S. Bauer, Flexible-foam-based capacitive sensor arrays for object detection at low cost. Appl. Phys. Lett. **92**, 013506 (2008). https://doi.org/10.1063/1.2830815
36. S. Chen, B. Zhuo, X. Guo, Large area one-step facile processing of microstructured elastomeric dielectric film for high sensitivity and durable sensing over wide pressure range. ACS Appl. Mater. Interfaces **8**, 20364–20370 (2016). https://doi.org/10.1021/acsami.6b05177
37. X. Shuai, P. Zhu, W. Zeng, Y. Hu, X. Liang, Y. Zhang, R. Sun, C. Wong, Highly sensitive flexible pressure sensor based on silver nanowires-embedded polydimethylsiloxane electrode with microarray structure. ACS Appl. Mater. Interfaces **9**, 26314–26324 (2017). https://doi.org/10.1021/acsami.7b05753
38. J. Lee, H. Kwon, J. Seo, S. Shin, J.H. Koo, C. Pang, S. Son, J.H. Kim, Y.H. Jang, D.E. Kim, T. Lee, Conductive fiber-based ultrasensitive textile pressure sensor for wearable electronics. Adv. Mater. **27**, 2433–2439 (2015). https://doi.org/10.1002/adma.201500009
39. K.A. Bijender, One-rupee ultrasensitive wearable flexible low-pressure sensor. ACS Omega **5**, 16944–16950 (2020). https://doi.org/10.1021/acsomega.0c02278
40. Bijender, A. Kumar, Flexible and wearable capacitive pressure sensor for blood pressure monitoring. Sens. Biosensing Res. **33**, 100434 (2021). https://doi.org/10.1016/J.SBSR.2021.100434
41. S. Kumar, Y.S. Bijender, A. Kumar, Flexible microhyperboloids facets giant sensitive ultra-low pressure sensor. Sens. Actuators A **328**, 112767 (2021). https://doi.org/10.1016/j.sna.2021.112767
42. M. Li, H. Jiang, D. Xu, D. Zhao, Z. Zhao, X. Dai, B. Lin, W.-X. He, L.-W. Jiang, Y. Zhang, Z. Lin, X. Huang, X. You, J. Ye, H. Wu, Highly sensitive capacitive pressure sensor with elastic metallized sponge. Smart Mater. Struct. **28**, 105023 (2019). https://doi.org/10.1088/1361-665X/AB3A0C
43. C. Dagdeviren, Y. Su, P. Joe, R. Yona, Y. Liu, Y.-S. Kim, Y. Huang, A.R. Damadoran, J. Xia, L.W. Martin, Y. Huang, J.A. Rogers, Conformable amplified lead zirconate titanate sensors with enhanced piezoelectric response for cutaneous pressure monitoring. Nat. Commun. **5**, 4496 (2014). https://doi.org/10.1038/ncomms5496
44. J. Chun, K.Y. Lee, C.-Y. Kang, M.W. Kim, S.-W. Kim, J.M. Baik, Embossed hollow hemisphere-based piezoelectric nanogenerator and highly responsive pressure sensor. Adv. Funct. Mater. **24**, 2038–2043 (2014). https://doi.org/10.1002/adfm.201302962
45. L. Persano, C. Dagdeviren, Y. Su, Y. Zhang, S. Girardo, D. Pisignano, Y. Huang, J.A. Rogers, High performance piezoelectric devices based on aligned arrays of nanofibers of poly(vinylidenefluoride-co-trifluoroethylene). Nat. Commun. **4**, 1633 (2013). https://doi.org/10.1038/ncomms2639
46. J.-H. Lee, H.-J. Yoon, T.Y. Kim, M.K. Gupta, J.H. Lee, W. Seung, H. Ryu, S.-W. Kim, Micropatterned P(VDF-TrFE) film-based piezoelectric nanogenerators for highly sensitive self-powered pressure sensors. Adv. Funct. Mater. **25**, 3203–3209 (2015). https://doi.org/10.1002/adfm.201500856
47. M. Akiyama, Y. Morofuji, T. Kamohara, K. Nishikubo, M. Tsubai, O. Fukuda, N. Ueno, Flexible piezoelectric pressure sensors using oriented aluminum nitride thin films prepared on polyethylene terephthalate films. J. Appl. Phys. **100**, 114318 (2006). https://doi.org/10.1063/1.2401312
48. C.-T. Lee, Y.-S. Chiu, Piezoelectric ZnO-nanorod-structured pressure sensors using GaN-based field-effect-transistor. Appl. Phys. Lett. **106**, 073502 (2015). https://doi.org/10.1063/1.4910879
49. C. Pan, L. Dong, G. Zhu, S. Niu, R. Yu, Q. Yang, Y. Liu, Z.L. Wang, High-resolution electroluminescent imaging of pressure distribution using a piezoelectric nanowire LED array. Nat. Photon. **7**, 752–758 (2013). https://doi.org/10.1038/nphoton.2013.191
50. L. Lin, Y. Xie, S. Wang, W. Wu, S. Niu, X. Wen, Z.L. Wang, Triboelectric active sensor array for self-powered static and dynamic pressure detection and tactile imaging. ACS Nano **7**, 8266–8274 (2013). https://doi.org/10.1021/nn4037514
51. F.R. Fan, L. Lin, G. Zhu, W. Wu, R. Zhang, Z.L. Wang, Transparent triboelectric nanogenerators and self-powered pressure sensors based on micropatterned plastic films. Nano Lett. **12**, 3109–3114 (2012). https://doi.org/10.1021/NL300988Z/SUPPL_FILE/NL300988Z_SI_002.AVI
52. J. Luo, F.R. Fan, T. Zhou, W. Tang, F. Xue, Z.L. Wang, Ultrasensitive self-powered pressure sensing system. Extreme Mech. Lett. **2**, 28–36 (2015). https://doi.org/10.1016/J.EML.2015.01.008
53. X. Wang, H. Zhang, L. Dong, X. Han, W. Du, J. Zhai, C. Pan, L. Wang, Self-powered high-resolution and pressure-sensitive triboelectric sensor matrix for real-time tactile mapping. Adv. Mater. **28**, 2896–2903 (2016). https://doi.org/10.1002/ADMA.201503407
54. L.Y. Chen, B.C.K. Tee, A.L. Chortos, G. Schwartz, V. Tse, D. Lipomi, H.S.P. Wong, M.V. McConnell, Continuous wireless pressure monitoring and mapping with ultra-small passive sensors for health monitoring and critical care. Nat. Commun. **5**, 1–10 (2014). https://doi.org/10.1038/ncomms6028
55. S. Yao, Y. Zhu, Wearable multifunctional sensors using printed stretchable conductors made of silver nanowires. Nanoscale **6**, 2345–2352 (2014). https://doi.org/10.1039/C3NR05496A
56. Z. Wang, L. Zhang, J. Liu, H. Jiang, C. Li, Flexible hemispheric microarrays of highly pressure-sensitive sensors based on breath figure method. Nanoscale **10**, 10691–10698 (2018). https://doi.org/10.1039/C8NR01495G
57. J. Heikenfeld, A. Jajack, J. Rogers, P. Gutruf, L. Tian, T. Pan, R. Li, M. Khine, J. Kim, J. Wang, J. Kim, Wearable sensors: modalities, challenges, and prospects. Lab Chip **18**, 217–248 (2018). https://doi.org/10.1039/C7LC00914C
58. C. Hou, H. Wang, Q. Zhang, Y. Li, M. Zhu, Highly conductive, flexible, and compressible all-graphene passive electronic skin for sensing human touch. Adv. Mater. **26**, 5018–5024 (2014). https://doi.org/10.1002/ADMA.201401367
59. B. Wang, T. Shi, Y. Zhang, C. Chen, Q. Li, Y. Fan, Lignin-based highly sensitive flexible pressure sensor for wearable electronics. J. Mater. Chem. C **6**, 6423–6428 (2018). https://doi.org/10.1039/C8TC01348A
60. H.-B. Yao, J. Ge, C.-F. Wang, X. Wang, W. Hu, Z.-J. Zheng, Y. Ni, S.-H. Yu, A flexible and highly pressure-sensitive graphene-polyurethane sponge based on fractured microstructure design. Adv. Mater. **25**, 6692–6698 (2013). https://doi.org/10.1002/adma.201303041
61. W. Yang, N.W. Li, S. Zhao, Z. Yuan, J. Wang, X. Du, B. Wang, R. Cao, X. Li, W. Xu, Z.L. Wang, C. Li, A breathable and screen-printed pressure sensor based on nanofiber membranes for electronic skins. Adv. Mater. Technol. **3**, 1700241 (2018). https://doi.org/10.1002/ADMT.201700241
62. S. Chen, K. Jiang, Z. Lou, D. Chen, G. Shen, Recent developments in graphene-based tactile sensors and E-skins. Adv. Mater. Technol. **3**, 1700248 (2018). https://doi.org/10.1002/ADMT.201700248
63. T. Dinh, T. Nguyen, H.P. Phan, N.T. Nguyen, D.V. Dao, J. Bell, Stretchable respiration sensors: advanced designs and multifunctional platforms for wearable physiological monitoring. Biosens. Bioelectron. **166**, 112460 (2020). https://doi.org/10.1016/J.BIOS.2020.112460
64. X. Wang, Y. Gu, Z. Xiong, Z. Cui, T. Zhang, X.W. Wang, Y. Gu, Z.P. Xiong, T. Zhang, Z. Cui, Silk-molded flexible, ultrasensitive,

and highly stable electronic skin for monitoring human physiological signals. Adv. Mater. **26**, 1336–1342 (2014). https://doi.org/10.1002/ADMA.201304248
65. Q. Yu, P. Zhang, Y. Chen, Human motion state recognition based on flexible, wearable capacitive pressure sensors. Micromachines **12**, 1219 (2021). https://doi.org/10.3390/MI12101219
66. Y. Ding, T. Xu, O. Onyilagha, H. Fong, Z. Zhu, Recent advances in flexible and wearable pressure sensors based on piezoresistive 3D monolithic conductive sponges. ACS Appl. Mater. Interfaces **11**, 6685–6704 (2019). https://doi.org/10.1021/ACSAMI.8B20929/ASSET/IMAGES/MEDIUM/AM-2018-20929N_0018.GIF
67. F. He, X. You, W. Wang, T. Bai, G. Xue, M. Ye, Recent progress in flexible microstructural pressure sensors toward human–machine interaction and healthcare applications. Small Methods **5**, 2001041 (2021). https://doi.org/10.1002/SMTD.202001041
68. Bijender, A. Kumar, Recent progress in the fabrication and applications of flexible capacitive and resistive pressure sensors. Sens. Actuators A Phys. **344**, 113770 (2022)
69. S. Mannsfeld, B. Tee, S. Barman, Z. Bao, Highly sensitive flexible pressure sensors with microstructured rubber dielectric layers. Nat. Mater. **9**, 859–864 (2010). https://doi.org/10.1038/nmat2834
70. W. Li, X. Jin, Y. Zheng, X. Chang, W. Wang, T. Lin, F. Zheng, O. Onyilagha, Z. Zhu, A porous and air gap elastomeric dielectric layer for wearable capacitive pressure sensor with high sensitivity and a wide detection range. J. Mater. Chem. C **8**, 11468–11476 (2020). https://doi.org/10.1039/D0TC00443J
71. Z. Zhang, X. Gui, Q. Hu, L. Yang, R. Yang, B. Huang, B.-R. Yang, Z. Tang, Highly sensitive capacitive pressure sensor based on a micropyramid array for health and motion monitoring. Adv. Electron. Mater. **7**, 2100174 (2021). https://doi.org/10.1002/AELM.202100174
72. I. Miranda, A. Souza, P. Sousa, J. Ribeiro, E.M.S. Castanheira, R. Lima, G. Minas, Properties and applications of PDMS for biomedical engineering: a review. J. Funct. Biomater. **13**, 2 (2021). https://doi.org/10.3390/JFB13010002
73. S. Baek, H. Jang, S.Y. Kim, H. Jeong, S. Han, Y. Jang, D.H. Kim, H.S. Lee, Flexible piezocapacitive sensors based on wrinkled microstructures: toward low-cost fabrication of pressure sensors over large areas. RSC Adv. **7**, 39420–39426 (2017). https://doi.org/10.1039/C7RA06997A
74. A. Chhetry, H. Yoon, J.Y. Park, A flexible and highly sensitive capacitive pressure sensor based on conductive fibers with a microporous dielectric for wearable electronics. J. Mater. Chem. C **5**, 10068–10076 (2017). https://doi.org/10.1039/C7TC02926H
75. Y. Jang, J. Jo, K. Woo, S.H. Lee, S. Kwon, H. Kim, H.S. Lee, Fabrication of highly sensitive piezocapacitive pressure sensors using a simple and inexpensive home milk frother. Phys. Rev. Appl. **11**, 014037 (2019). https://doi.org/10.1103/PhysRevApplied.11.014037
76. C. Xin, L. Chen, T. Li, Z. Zhang, T. Zhao, X. Li, J. Zhang, Highly sensitive flexible pressure sensor by the integration of microstructured PDMS Film with a-IGZO TFTs. IEEE Electron. Device Lett. **39**, 1073–1076 (2018). https://doi.org/10.1109/LED.2018.2839595